Available online at www.sciencedirect.com
SCIENCE DIRECT®
Journal of Photochemistry and Photobiology A: Chemistry 160 (2003) 105–114
Journal of Photochemistry and Photobiology A:Chemistry
www.elsevier.com/locate/jphotochem

Photocatalytic oxidation of toluene on irradiated TiO_2: comparison of degradation performance in humidified air, in water and in water containing a zwitterionic surfactant

G. Marcì [a], M. Addamo [a], V. Augugliaro [a], S. Coluccia [b], E. García-López [a], V. Loddo [a], G. Martra [b], L. Palmisano [a,*], M. Schiavello [a]

[a] *Dipartimento di Ingegneria Chimica dei Processi e dei Materiali, Università degli Studi di Palermo, Viale delle Scienze, 90128 Palermo, Italy*
[b] *Dipartimento di Chimica IFM, Università degli Studi di Torino, Via Pietro Giuria 7, 10125 Torino, Italy*

Received 7 January 2003; received in revised form 31 January 2003; accepted 10 April 2003

Abstract

Photocatalytic degradation of toluene was carried out both in gas–solid and in liquid–solid regime by using polycrystalline samples of TiO_2 Merck and TiO_2 Degussa P25. For the gas–solid regime two types of continuous photoreactor were used, a fixed bed one of cylindrical shape and a Carberry type photoreactor, both irradiated by near-UV light. The inlet reacting mixture consisted of air containing toluene and water vapours. The influence of the gas flow rate and the presence of water vapour on the photocatalytic process was investigated. CO_2 and benzaldehyde were the toluene degradation products detected in the gas phase by using TiO_2 Merck. In the presence of water vapour this catalyst exhibited a stable activity, which greatly decreased in the absence of water vapour. On the contrary, TiO_2 Degussa P25 produced CO_2 and traces of benzaldehyde but it continuously deactivated even in the presence of water vapour. For the liquid–solid regime a batch photoreactor with immersed lamp was used. In order to increase the reaction rate, a zwitterionic surfactant, i.e. tetradecyldimethylamino-oxide, was added to the reacting mixture. A complete photo-oxidation of toluene was achieved after few hours of irradiation in the presence of both types of photocatalysts; longer irradiation times produced the photodegradation of surfactant. The main intermediates of toluene degradation were *p*-cresol and benzaldehyde while traces of pyrogallol and benzyl alcohol were also found. Benzoic acid, hydroquinone and *trans*, *trans*-muconic acid were detected only with TiO_2 Merck. The reaction rate was higher in the presence of the surfactant suggesting that this compound acts as a sequestration agent. An FTIR study gave information on the role played by superficial hydroxyl groups both on the onset of activity and on the deactivation process. On the basis of photoreactivity results and of FTIR investigation the differences of activity and distribution and nature of toluene degradation products are critically discussed for the three reacting systems used.

Keywords: Toluene degradation; Heterogeneous photocatalysis; TiO_2; Sequestrating agent; FTIR

1. Introduction

Heterogeneous photocatalysis in the presence of semiconductor oxides is a fast growing field of basic and applied research, especially for the case of the oxidation of organic pollutants in water [1–3] or in air [4–6]. In particular, photocatalytic oxidation offers various advantages compared with traditional treatment methods because the photoreactions occur at room temperature and atmospheric pressure, under radiation of the near-UV region and at measurable rates [7] until to very low concentration levels.

Toluene is a widespread reagent used for the preparation of many compounds, such as benzaldehyde, benzyl alcohol, benzoic acid, chloro derivatives, etc. and consequently it can be found in many industrial waste effluents. Toluene is a very noxious organic compound and many strategies have been identified to reduce its presence in the environment.

Heterogeneous photocatalytic method has been tested for toluene abatement and previous papers report the partial or complete oxidation of toluene both in gas–solid [8–13] and in liquid–solid systems [14–17].

As to concern the gas–solid regime, Ibusuki and Takeuchi [8] carried out the complete photo-oxidation of toluene on TiO_2 at room temperature. They found that the presence of water vapour was beneficial in order to achieve the almost complete mineralisation of toluene, benzaldehyde having

* Corresponding author. Tel.: +39-091-656-7246; fax: +39-091-656-7280.
E-mail address: palmisano@dicpm.unipa.it (L. Palmisano).

1010-6030/03/$ – see front matter © 2003 Elsevier Science B.V. All rights reserved.
doi:10.1016/S1010-6030(03)00228-4

been detected only in very small amounts. However, the product distribution and the catalyst stability strongly depend on the nature of the catalyst and the experimental conditions. Furthermore, Obee and Brown [9] studied the influence of the competitive adsorption of water and toluene vapours on the photo-oxidation rate. Luo and Ollis [10] and Einaga et al. [11], by studying the toluene degradation in humidified air, report that the influence of water is complex in the sense that an optimum water concentration was found for which a maximum of reactivity was observed. In any case no significant amounts of intermediate species were detected. Recently the selective photo-oxidation of gaseous toluene to benzaldehyde on TiO_2 powders has been reported as an effective method to transform this compound to a valuable chemical [12,13]. Moreover, Cao and coworkers [14] reported the photocatalytic oxidation of toluene by using nanostructured TiO_2 catalysts. They found a severe deactivation of TiO_2 due to the accumulation of partially oxidised intermediates. The complete recovery of catalytic activity required a thermal treatment of the photocatalysts at a temperature above 420 °C.

For liquid–solid systems, Fujihira et al. [15,16] studied the photo-oxidation of toluene in aqueous aerated suspensions containing various powdered semiconductors. They reported the formation of cresols, benzaldehyde and benzyl alcohol, depending on the pH of the solution and on the used semiconductor. The formation of benzaldehyde was also confirmed by Navio et al. [17], which used acetonitrile as solvent and investigated the influence of the presence of water on the products distribution. Recently the use of a surfactant to enhance the photocatalytic reaction rate for toluene degradation has been reported [18]. The presence of surfactants or humic acids was found beneficial for degrading various substrates and a sequestration effect has been hypothesised [19,20] for explaining this effect.

Mechanistic aspects of the partial photo-oxidation of toluene in gas–solid regime and the role of the presence of water vapour in those systems have been also investigated by FTIR spectroscopy [8,13].

In this work the photocatalytic degradation of toluene in gas–solid and in liquid–solid regime has been carried out by using two different types of commercial polycrystalline TiO_2. For the gas–solid regime, the influence on the reaction of some parameters such as toluene concentration, water presence and gas flow rate was investigated. For the liquid–solid regime, a kinetic and mechanistic investigation has been performed. In order to enhance the toluene photodegradation rate, tetradecyldimethylamino-oxide, a zwitterionic surfactant, was added to the reacting mixture. The behaviour of toluene–surfactant mixtures appears to be worth of attention, not only by a scientific point of view but also because some actual civil or industrial wastewater contain both compounds. Analyses of the main intermediates products were carried out by HPLC and they were compared with those detected in the gas–solid system.

For obtaining information on the interactions between reactants and photo-oxidation products at the surface of the photocatalysts, an FTIR study of the adsorption of toluene and benzaldehyde with the two types of TiO_2 powders employed was carried out.

2. Experimental

2.1. Gas–solid system

Fig. 1 shows the set-up used for carrying out the experimental runs. Two photoreactors were used: the first one (Fig. 2a) was a Pyrex photoreactor of cylindrical shape (internal diameter: 5 cm, external diameter: 5.4 cm, height: 10 cm). A porous glass septum on the bottom of the cylinder allowed to sustain the fixed bed and to distribute the inlet gaseous mixture. The reactor was vertically positioned inside a thermostated chamber of 20 cm diameter and 35 cm deep and irradiated from the top by a 400 W medium pressure Hg lamp (Polymer GN ZS, Helios Italquartz) placed at a distance of 12 cm from the top of catalyst bed. The irradiated surface of the bed was 19.6 cm^2. The radiant energy impinging on the reactor was measured at $\lambda = 360$ nm by using a radiometer UVX Digital; its value was 4.5 mW cm^{-2}. The temperature inside the photoreactor was ca. 403 K. The gas flow rates ranged from 0.020 to 0.250 $cm^3\ s^{-1}$. Toluene and water concentrations in the feed were 0.030 and 0.75 mM, respectively.

The catalysts used were commercial polycrystalline TiO_2 Merck (≈100% anatase, BET surface area: 10 $m^2\ g^{-1}$) and TiO_2 Degussa P25 (≈80% anatase, ≈20% rutile, BET surface area: 50 $m^2\ g^{-1}$).

The reactivity runs were carried out with different masses of catalyst but at equal surface area, 100 m^2; therefore 10 g for TiO_2 Merck or 2 g for TiO_2 Degussa P25. The corresponding fixed bed heights were ca. 1 and 2 cm, respectively.

The second photoreactor was a Carberry type one (Fig. 2b); it had the shape of rectangular parallelepiped (30 cm × 30 cm × 24 cm, free volume: 16.3 dm^3) with four Pyrex windows (17 cm × 15 cm) in the vertical walls. Inside the photoreactor a spinning basket was placed (Fig. 2c); it consisted of four blades of small nets that were coated by the catalyst (TiO_2 Merck, ca. 60 g). The photoreactor was thermostated by using power resistances to ca. 403 K. The catalyst was illuminated through the wall windows by using four sets of three fluorescent lamps (Philips Eversun, 16 W) positioned 10 cm far from the windows. The average impinging photon flow, measured at the surface of one blade of the spinning basket, was 1 mW cm^{-2}. The total irradiated geometrical surface was 864 cm^2. Toluene and water concentrations were held constant at 0.0055 and 0.75 mM, respectively and the gas flow rate was 33.3 $cm^3\ s^{-1}$.

The procedure of the photoreactivity runs was always the same. The gas fed to the photoreactor consisted of air, toluene and water. The last two compounds were introduced

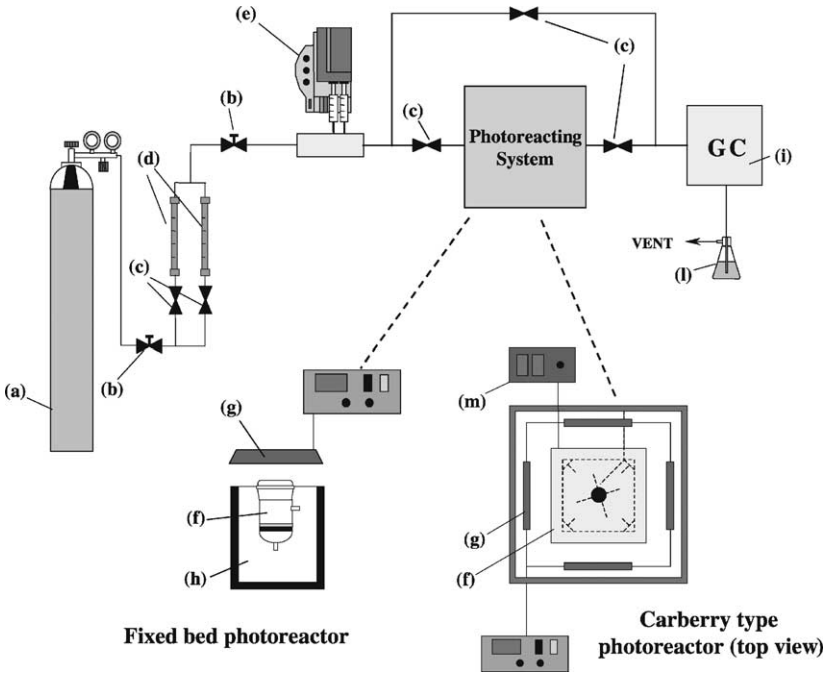

Fig. 1. Experimental set-up used for the gas–solid experiments. (a) Air cylinder; (b) control valves; (c) switch valves; (d) rotameters; (e) infusion pump; (f) photo-reactor; (g) irradiation system; (h) oven; (i) gas chromatograph with an FID detector; (l) bubbling bottle containing saturated barium hydroxide aqueous solution to trap CO_2; (m) temperature control system.

in the air stream by means of an infusion pump. The irradiation started only when steady-state conditions were achieved, i.e. after about 24 h of gas feeding. The runs lasted ca. 24 h and the gas at the exit of the photoreactor was periodically analysed by a gas chromatograph (Hewlett-Packard 6890) equipped with an FID detector and an Alltech Carbograph column (2 mm long × 2 mm i.d.). For some experiments the outlet gas was continuously bubbled in a trap containing pure water that was analysed at the end of the run by HPLC. A Varian 9010 Solvent Delivery System coupled with a Varian 9050 variable wavelength UV-Vis detector was used with an Alltech Alltima column C18 5 μm (250 mm long × 4.6 mm i.d.), eluent methanol/H_3PO_4 (0.05% in water 45/55, v/v). For selected runs the outlet gas was bubbled in a saturated aqueous solution of barium hydroxide, in order to trap CO_2 as barium carbonate.

At the end of each run the used catalyst was put in acetonitrile for 1 h; the resulting solution was analysed by HPLC after separation of the solid by filtration through 0.45 μm cellulose acetate filter (HA, Millipore).

2.2. Liquid–solid system

A Pyrex batch photoreactor of cylindrical shape containing 1.5 l of aqueous suspension was used for performing the photoreactivity experiments. The photoreactor was provided with ports in its upper section for the inlet and outlet of gases, for sampling and for pH and temperature measurements. A magnetic stirrer guaranteed a satisfactory suspension of the photocatalyst and the uniformity of the reacting mixture which was saturated by bubbling pure oxygen at atmospheric pressure for 0.5 h before switching on the lamp. The gas was continuously bubbled also during the runs that lasted a time ranging from 1.5 to 10 h. A 500 W medium pressure Hg lamp (Helios Italquartz) was immersed within the photoreactor; the lamp was cooled by water circulating through a Pyrex jacket and the suspension had a temperature of about 300 K. The radiation energy impinging on the suspension had an average value of 19.3 mW cm^{-2}. For all the runs the catalyst amount was 0.4 g l^{-1} and the initial pH of the suspension was equal to 6.0. Initial toluene concentrations were in the 0.1–1.4 mM range; the highest concentration is well below the solubility limit of toluene in water that is 5.4 mM at room temperature.

In order to enhance the toluene photodegradation rate, tetradecyldimethylamino-oxide (C_{14}DMAO), a zwitterionic surfactant whose formula is reported below

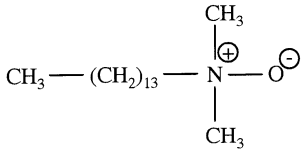

was added to the reacting mixture. The surfactant concentration was 0.05 mM for the majority of the runs. The molar ratios between toluene and C_{14}DMAO varied from 2 to 28. Some experiments were carried out by using a surfactant concentration in the 0.01–0.075 mM range and an initial toluene concentration of 0.37 mM.

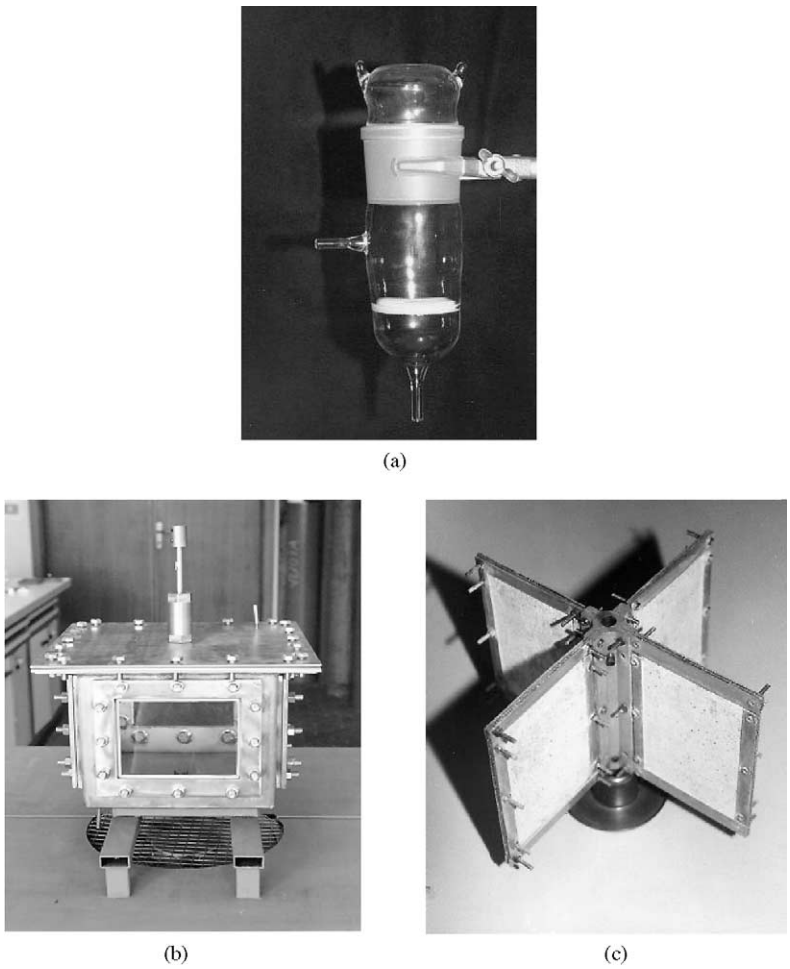

Fig. 2. Pictures of the: (a) fixed bed photoreactor; (b) Carberry type photoreactor and (c) spinning basket containing the photocatalyst.

Toluene and its intermediate oxidation products were analysed by HPLC. The analyses were performed after separation of the catalyst by filtration. For the runs carried out in the absence of surfactant, before the separation of the catalyst a very small amount of surfactant was added to the withdrawn sample in order to improve its homogeneity. Two different Alltech columns were used: an Econosphere C18 3 μm (150 mm long × 4.6 mm i.d.) with an eluent acetonitrile/water 35/65 (v/v) to analyse toluene and an Econosil C18 10 μm (250 mm long × 4.6 mm i.d.) with eluent acetonitrile/water 65/35 (v/v) to analyse the other products.

Total organic carbon (TOC) analyses were carried out for all the runs by using a 5000A Shimadzu TOC analyser in order to check the complete mineralisation both of toluene and surfactant. It was not possible to determine confidently the C_{14}DMAO concentration; the fate of the surfactant was therefore followed only by TOC analysis.

2.3. FTIR study

For the IR measurements, the TiO_2 powder was pressed in the form of self-supporting pellets (40 mg cm^{-2}) and then placed in a IR quartz cell, equipped with KBr windows, connected to a conventional vacuum line (residual pressure: 1.33×10^{-4} Pa) allowing all adsorption–desorption to be carried out in situ. The IR spectra (4 cm^{-1} resolution) of TiO_2 self-supporting pellets were recorded with a Bruker IFS 48 spectrometer both in the absence and in the presence of adsorbed reacting species. High purity toluene and benzaldehyde (Sigma Aldrich) were admitted onto the samples after several freeze–pump–thaw cycles.

3. Results and discussion

For both gas–solid and liquid–solid regimes blank reactivity tests were performed under the same experimental conditions used for the photoreactivity experiments but in the absence of catalyst, oxygen or light. No reactivity was observed in all these cases so that it was concluded that the contemporary presence of O_2, catalyst and irradiation is needed for the occurrence of toluene degradation process.

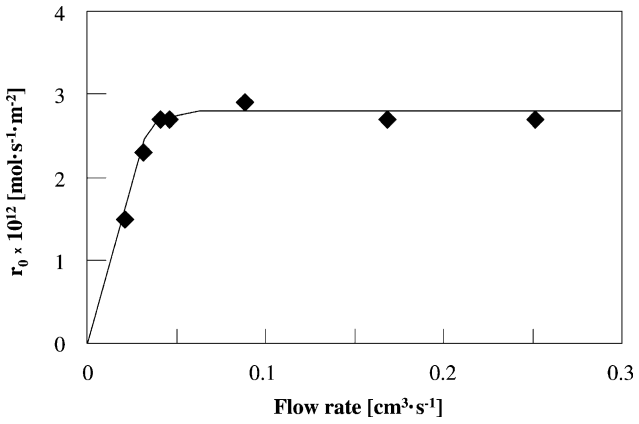

Fig. 3. Fixed bed photoreactor: toluene disappearance rate per square meter of catalyst (r_0) versus the gas flow rate. Inlet toluene concentration: 0.030 mM, water vapour concentration: 0.75 mM.

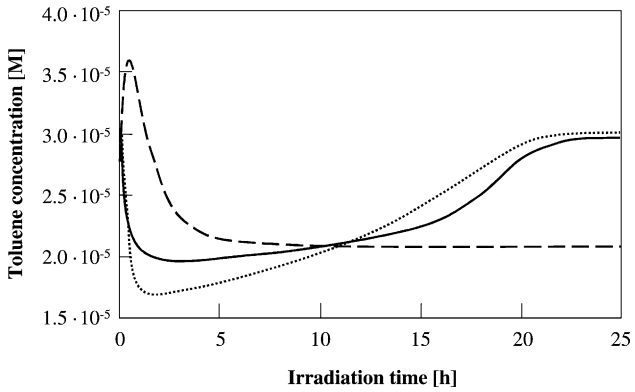

Fig. 4. Fixed bed photoreactor: experimental results of outlet toluene concentration versus irradiation time by using TiO_2 Degussa P25 in the presence of water (···) and TiO_2 Merck in the presence (- - -) or in the absence (—) of water vapour. Flow rate: 0.045 cm^3 s^{-1}; inlet toluene concentration: 0.030 mM, water vapour concentration: 0.75 mM.

3.1. Gas–solid system: fixed bed photoreactor

Preliminary tests were performed with the aim of determining suitable flow rate conditions to avoid mass transport limitations on the photoreaction. Fig. 3 reports the toluene disappearance rates per square meter of photocatalyst (r_0) versus the gas flow rate. An enhancement of the reaction rate may be observed for flow rates up to ca. 0.040 cm^3 s^{-1}; for higher values the reaction rate did not change significantly. The above finding indicates that mass transfer resistance limits the reaction rate for flows lower than 0.040 cm^3 s^{-1}. On this ground all the photocatalytic experiments were carried out in the 0.045–0.250 cm^3 s^{-1} flow rate range. In order to check that all the fixed bed was irradiated, i.e. that the penetration depth of radiation was higher that the height of the fixed bed, a few runs were carried out with higher amounts of TiO_2 Merck catalyst. It was found an increase of activity by increasing the catalyst amount so that it was concluded that at the usual bed height (1 cm) all the catalyst particles were irradiated.

Fig. 4 reports the values of outlet toluene concentration versus irradiation time for three representative runs; in this figure for the sake of clarity the experimental points have been substituted by interpolating lines. The three runs were carried out with the same inlet toluene concentration in the presence of water vapour with TiO_2 Merck and TiO_2 Degussa P25 and in the absence of water vapour with TiO_2 Merck. The oxidation products detected both in the gas phase and on the catalyst surface are reported in Table 1.

In the presence of water vapour for TiO_2 Merck there is a fast increase of outlet toluene concentration after switching on the lamp, followed by a slow decrease down to a steady value less than the inlet one. A maximum conversion of ca. 24%, corresponding to an oxidation rate of 2.7×10^{-12} mol s^{-1} m^{-2}, was achieved at steady-state conditions. The main photo-oxidation products detected in the gas phase were carbon dioxide and benzaldehyde. The results of benzaldehyde concentration versus irradiation time for a representative run are reported in Fig. 5. It can be noticed that the benzaldehyde concentration reaches a maximum after 3–4 h of irradiation and therefore it slightly decreases reaching a steady value after ca. 7 h.

For TiO_2 Degussa P25 the outlet toluene concentration shows a sharp decrease followed by a slow increase up to the inlet value thus indicating the occurrence of deactivation. The main oxidation product was carbon dioxide; benzaldehyde was detected in very small quantities while high

Table 1
Intermediates detected in liquid–solid regime and in gas–solid regime

Intermediates	TiO_2 Merck		TiO_2 Degussa P25	
	Liquid–solid	Gas–solid	Liquid–solid	Gas–solid
p-Cresol (4-methylphenol)	Yes	No	Yes	No
Benzaldehyde	Yes	Yes	Yes	Yes
Benzyl alcohol	Yes	Yes[a]	Yes	Yes[a]
Benzoic acid	Yes	Yes[a]	No	Yes[a]
Pyrogallol (1,2,3-trihydroxybenzene)	Yes	No	Yes	No
Hydroquinone	Yes	No	No	No
Trans, trans-muconic acid (*trans,trans*-2,4-esadiendioic acid)	Yes	No	No	No

[a] Product found as adsorbed species onto the catalyst surface at the end of the run.

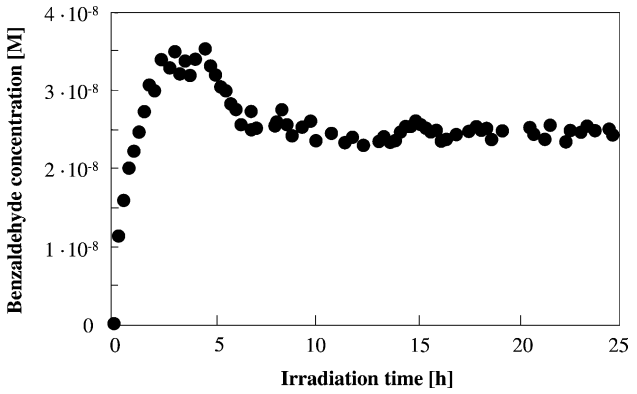

Fig. 5. Fixed bed photoreactor: experimental results of outlet benzaldehyde concentration versus irradiation time by using TiO_2 Merck. Gas flow rate: 0.045 $cm^3\,s^{-1}$; inlet toluene concentration: 0.030 mM; water vapour concentration: 0.75 mM.

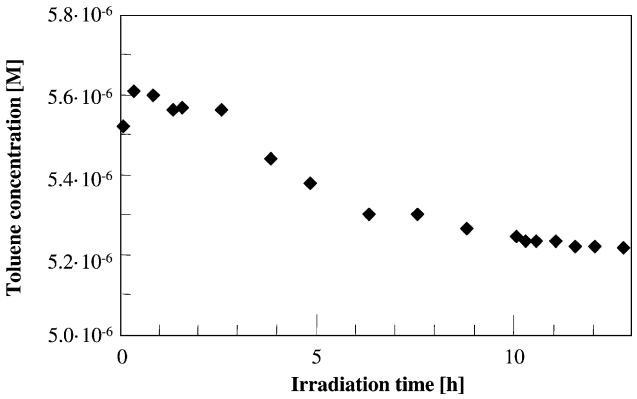

Fig. 6. Carberry type photoreactor: experimental results of outlet toluene concentration versus irradiation time by using TiO_2 Merck. Gas flow rate: 33.3 $cm^3\,s^{-1}$; inlet toluene concentration: 0.0055 mM; water vapour concentration: 0.75 mM.

amounts of benzoic acid were found adsorbed onto the catalyst surface.

The absence of water greatly affects the performance of TiO_2 Merck catalyst as it continuously deactivates. Indeed, a maximum conversion of 33.5% (corresponding to an oxidation rate of 4.2×10^{-12} mol s^{-1} m^{-2}) was reached after ca. 2 h. After that, the photoreactivity continuously decreased down to negligible values. The initial decrease of outlet toluene concentration, however, was more significant than that observed in the presence of water vapour. This finding can be explained by considering that the absence of water vapour favours the adsorption of toluene on the catalyst surface. In addition the desorption of benzaldehyde is more difficult when water is absent and this could induce the deactivation of the photocatalyst. Indeed, benzaldehyde remaining adsorbed on the catalyst surface can be more easily attacked by oxidant radical species and transformed into benzoic acid that strongly interacts and occupies surface sites.

3.2. Gas–solid system: Carberry type photoreactor

The main drawback of the fixed bed photoreactor is that it cannot process high flow rates. In this case, in fact, the pressure drop reaches very high values and, in addition, the phenomenon of particle drag can occur. In order to test the photocatalytic process at high flow rate overcoming the previous disadvantages, a few experimental runs were carried out by using a Carberry type photoreactor. This type of photoreactor, due to its particular engineering, overcomes the previous drawbacks and in addition shows the advantage that the mass transport resistances play a very negligible role thus allowing also the treatment of very low flow rates.

In Fig. 6 the experimental values of outlet toluene concentration versus irradiation time are reported for a run carried out in the presence of TiO_2 Merck at a flow rate (33.3 $cm^3\,s^{-1}$) two orders of magnitude higher than that usually used in the fixed bed photoreactor. The photoreactivity results indicate that the reactor reaches steady-state conditions after ca. 10 h from the beginning of the irradiation. During the first 3 h, the outlet toluene concentration was higher than that of the inlet; owing to the very high amount of catalyst present in the photoreactor a high amount of toluene was adsorbed in the dark so that its photodesorption under irradiation justifies the previous finding. At the used experimental conditions the conversion of toluene was ca. 5%. At steady-state conditions the reacted toluene was almost completely mineralised because the carbon balance was satisfied in the limits of experimental errors by the produced CO_2; only traces of benzaldehyde and benzoic acid were detected.

The parameter used to compare the results obtained with the Carberry photoreactor with those of the fixed bed was the reaction rate per unit of photon energy (at 360 nm) impinging on the geometric irradiated surface. The values of these reactions rate were 3.06×10^{-5} and 9.60×10^{-5} mol s^{-1} W^{-1} for the fixed bed and the Carberry type photoreactor, respectively. It can be noticed that the values of the reaction rate are of the same order of magnitude, thus indicating that the Carberry photoreactor shows an efficiency similar to that of the fixed bed one at the very high flow rate used.

3.3. Liquid–solid system

As reported in Section 2, the photocatalytic degradation of toluene was also performed in liquid phase. In order to enhance the degradation rate some runs were carried out by adding to the liquid phase variable amounts of C_{14}DMAO surfactant. Blank tests carried out in the absence of catalyst with toluene:C_{14}DMAO molar ratio equal to 6:1 indicated that only a slight decrease of toluene concentration occurred even after 2 h of irradiation; for these runs the TOC content did not change with time. No investigation was carried out in order to identify the aggregated systems present in the homogeneous media even if it is possible to state that toluene–surfactant interaction is hydrophobic in nature.

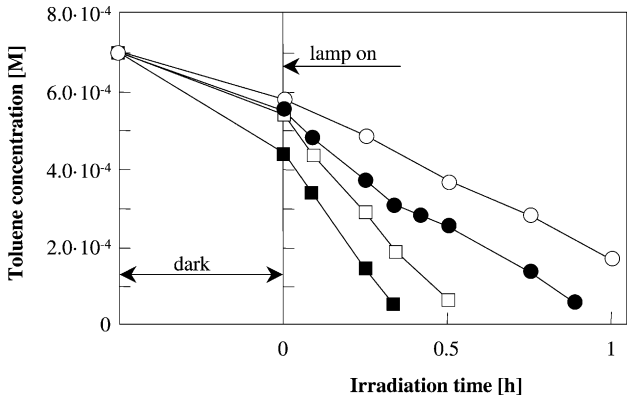

Fig. 7. Experimental results of toluene concentration versus irradiation time for runs carried out in batch liquid–solid photoreactor without (□) and with (■) C_{14}DMAO by using TiO_2 Degussa P25 (0.4 g l^{-1}) and without (○) and with (●) C_{14}DMAO by using TiO_2 Merck (0.4 g l^{-1}). Toluene:C_{14}DMAO molar ratio 14:1.

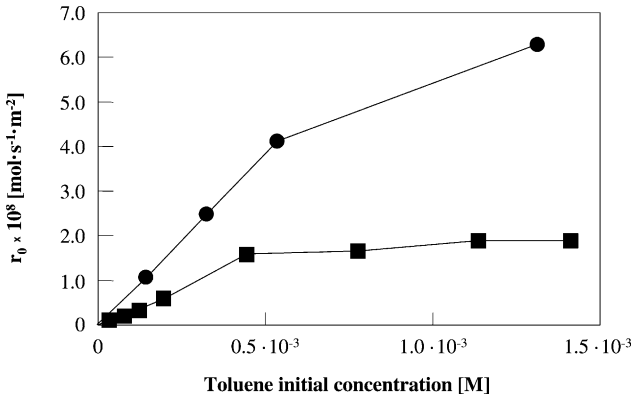

Fig. 9. Initial reaction rate of toluene disappearance per square meter of catalyst (r_0) versus toluene initial concentration. C_{14}DMAO concentration: 0.05 mM; TiO_2 Merck (●); TiO_2 Degussa P25 (■).

Fig. 7 reports experimental data of toluene concentration versus irradiation time for runs carried out without the addition of surfactant. Toluene concentration values measured after 30 min of mixing in the dark showed a decrease with respect to initial ones indicating the occurrence of physical adsorption. The amount of adsorbed toluene was higher for TiO_2 Degussa P25 than for TiO_2 Merck; this feature can be explained by considering the different values of surface area of the catalysts. Fig. 7 also reports photoreactivity data obtained in the presence of surfactant. It may be noted that the addition of surfactant determines a more significant decrease of the concentration of toluene in the liquid phase at the start of irradiation. This behaviour can be explained by hypothesising a sequestrating effect of the surfactant which traps the toluene molecules close to the catalytic surface. It is worth noticing that this phenomenon was more relevant for TiO_2 Degussa P25. All the photoreactivity runs carried out in the presence of C_{14}DMAO showed that the surfactant enhances the toluene degradation rate for both catalysts. Moreover, ca. 40 mol% of surfactant was degraded during the runs, while for its complete mineralisation longer times were needed depending on the experimental conditions used.

Fig. 8 reports the concentration values of toluene and of the main intermediate products (*p*-cresol and benzaldehyde) detected during a photodegradation run carried out in the presence of surfactant. From the observation of data reported in Fig. 8 it may be noted that the slopes at zero time of lines interpolating the data of intermediates concentrations are different from zero. This feature clearly indicates that *p*-cresol and benzaldehyde are produced through independent reactions in parallel involving toluene. The slope of toluene disappearance curve at zero time is quite higher than the sum of slopes of intermediates production. This feature indicates that there is a third pathway, in parallel with the previous ones, by which toluene is transformed to the main oxidation product detected, i.e. CO_2. It is worth reporting that the presence of the surfactant does not affect the intermediates distribution in the reacting medium.

As a kinetic modelling of the reactivity results is out of the aims of the present work, the comparison of the different surfactant–toluene systems has been carried out by using the initial degradation rate of toluene. In Fig. 9 the values of the

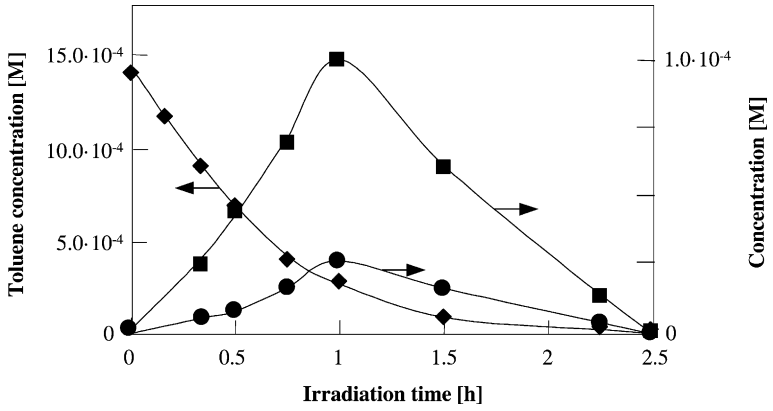

Fig. 8. Experimental results of toluene (◆); *p*-cresol (■) and benzaldehyde (●) concentrations versus irradiation time for a run carried out in batch liquid–solid photoreactor by using TiO_2 Degussa P25 (0.4 g l^{-1}). Toluene:C_{14}DMAO molar ratio 28:1.

initial reaction rate referred to the catalyst surface area, r_0, are reported versus the toluene concentration at the start of irradiation, with the same C_{14}DMAO amount, by using both catalysts. It can be observed that the r_0 values increase by increasing the toluene concentration for both catalysts. When TiO_2 Degussa P25 was used, the r_0 values show the typical Langmuir pattern with an almost constant value of r_0 for toluene concentration values higher than 0.5×10^{-3} M thus suggesting the achievement of a complete monolayer coverage above this value. On the contrary, when TiO_2 Merck was used, the monotone increase of r_0 with the toluene concentration indicates an incomplete coverage of toluene on the catalyst surface even at the highest concentration used.

The r_0 values increased about 50% for TiO_2 Merck and about 20% for TiO_2 Degussa P25 on respect to the corresponding runs carried out without surfactant. These results confirm the occurrence of a sequestrating effect by the surfactant. For TiO_2 Merck this effect is strong as the catalyst exhibits a low coverage of toluene while for TiO_2 Degussa P25 the presence of surfactant does not affect appreciably the initial reaction rate because the coverage of the surface is almost complete.

The order of magnitude of toluene photodegradation rate in liquid phase is of 10^{-8} mol s^{-1} m^{-2} while in gas phase is of 10^{-12} mol s^{-1} m^{-2}; therefore the rate in liquid phase is 10^4 times higher than that in gas phase. It is known that the photodegradation kinetics is affected by the radiation intensity and by the reagent concentrations. In the present case the photon energy impinging the catalyst surface was of the same order of magnitude for both systems. The photoreactivity results here reported show that water is an essential reagent for the occurrence of reaction. For the gas system the orders of magnitude of toluene and water concentrations were 10^{-5} and 10^{-4} M while for the liquid system they were 10^{-4} and 55 M, respectively. Therefore in the liquid phase the concentration of reagents is about 10^6 times higher than that in gas phase. It is likely that this huge difference in reagent concentration could be responsible of the observed difference of photoreactivity between the liquid and the gas phase.

3.4. FTIR investigation

Fig. 10 reports the IR spectra of TiO_2 Merck (A) and TiO_2 Degussa P25 (B) related to their interaction with toluene. At first, the two photocatalysts have been simply outgassed at room temperature, in order to leave on their surface a full monolayer of hydroxyl groups and water molecules coordinated to surface Ti^{4+} ions. This monolayer is expected to correspond to the first surface hydration layer in both the gas–solid and liquid–solid regimes adopted for performing photoreactivity tests.

In this condition, the spectra of both TiO_2 powders (curves a) exhibit a series of components in the 3700–3600 cm^{-1} range, due to the stretching mode (ν) of vibrationally free hydroxyl groups and a broad and complex absorption, spread

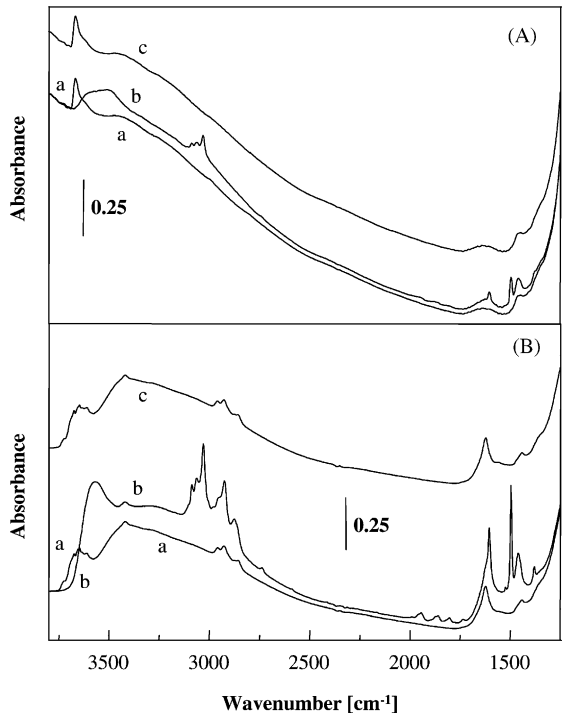

Fig. 10. IR spectra of TiO_2 Merck (A) and TiO_2 Degussa P25 (B): (a) outgassed at room temperature for 45 min; (b) in contact with 3.0 Torr of toluene; (c) after 5 min re-outgassing at room temperature.

on the 3600–2600 cm^{-1} range, resulting from the superposition of the ν_{OH} mode of hydrogen bonded hydroxyl groups and the symmetric and antisymmetric ν_{OH} modes of water molecules coordinated to surface Ti^{4+} surface ions [21].

The reachness in components of the absorption related to the vibrationally free hydroxyl groups of TiO_2 P25 (Fig. 10A, curve a) can be ascribed to the higher surface heterogeneity, in terms of types of surface planes and defect positions (steps, edges, corners), of this material with respect TiO_2 Merck [21].

At lower frequency, the weaker bands at 1620 and 1450–1350 cm^{-1} can be assigned to the bending mode of water molecules coordinated to surface Ti^{4+} ions and to carbonate-like groups, respectively [22], the latter produced by reaction of CO_2 with basic surface centres during the storage of the catalysts in air.

For both TiO_2 powders, the ν_{OH} bands in the 3700–3600 cm^{-1} range completely disappear by admission of toluene and are transformed in an intense and broad components centred at ca. 3500 cm^{-1} (Fig. 10A and B, curves b). This behaviour clearly indicates that vibrationally free hydroxyls act as effective Lewis acid adsorption sites for toluene, the observed shift resulting from the interaction between such OH groups and the π electrons of the aromatic molecules [23]. At lower frequencies, peaks due to adsorbed toluene appear in the 3100–2800 cm^{-1} (CH stretchings) and 1610–1360 cm^{-1} (ring stretchings, CH deformations) ranges.

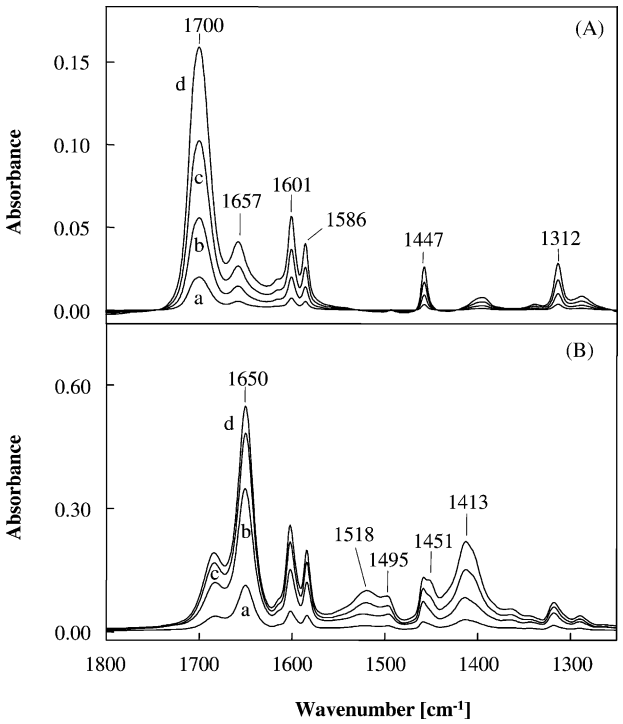

Fig. 11. IR spectra of benzaldehyde adsorbed under increasing pressure on TiO_2 Merck (A) and TiO_2 Degussa P25 (B) both outgassed at room temperature for 45 min: (a) 0.5 Torr; (b) 1.9 Torr; (c) 2.0 Torr and (d) 3.0 Torr.

The bands of adsorbed toluene disappear and the original spectral features of the vibrationally free OH groups are completely restored after short outgassing at room temperature (Fig. 10A and B, curves c), indicating that, for both catalysts, the interaction between the aromatic molecules and hyroxyl groups is very weak.

Conversely, the interaction of benzaldehyde with the surface of the photocatalyst exhibits a significant dependence on the type of TiO_2 photocatalyst. In the case of TiO_2 Merck, adsorbed benzaldehyde produced an IR spectrum characterised by a main peak at 1700 cm^{-1} and bands at 1657, 1601, 1586, 1447 and 1312 cm^{-1} (Fig. 11A). This spectral pattern is very similar to that exhibited by benzaldehyde in CCl_4 solution, suggesting that aldehyde molecules are adsorbed on the surface of the catalyst essentially in a weakly perturbed form, through hydrogen bonding with surface hydroxyl groups.

The adsorption of benzaldehyde on TiO_2 P25 produced a significantly different spectral pattern. In this case the components due to benzaldehyde molecules adsorbed in an unperturbed form were observed as minor features and the IR spectrum appeared dominated by new component, such as an intense peak at 1650 cm^{-1} and a series of bands at 1518, 1495, 1451 and 1413 cm^{-1} (Fig. 11B). The main peak at 1650 cm^{-1} and the other new bands at lower frequency could be assigned to hemiacetalic-like species formed by nucleophilic attack of basic oxygen of hydroxyl species to the carbon atom of the carbonyl group of adsorbed aldehyde molecules, as in the first step of the Cannizzaro reaction.

Such a difference in the interaction towards benzaldehyde results from the differences in morphology and surface structure of the two types of TiO_2 powders used [20]. These differences also affect the reactivity of the hydroxyl groups, present in high hydration conditions, which behave as electron acceptor (through the H atom) in the case of TiO_2 Merck, while exhibit a nucleophilic character (through the O atom) for TiO_2 Degussa P25.

This different chemical behaviour could well account for the different photocatalytic behaviour exhibited by the two types of TiO_2 powders in wet reaction feed. In the case of TiO_2 Merck, benzaldehyde molecules resulting from the photo-oxidation of toluene weakly interact with the catalyst surface so that they can be released to the gas phase.

By contrast, hydroxyl groups on the surface of TiO_2 P25 are able to react with photo-produced benzaldehyde, which is then retained on the catalyst surface. Subsequently it can be converted in other products, like benzoic acid, strongly adsorbed on the TiO_2 surface leading to the progressive deactivation of the catalyst in the gas–solid system. Deactivation was not observed in liquid–solid system probably because liquid water is able to displace the benzaldehyde from the catalyst surface.

As for the deactivation of TiO_2 Merck when a dry reaction feed was used, previous studies indicated that this behaviour should result from an irreversible consumption of surface hydroxyl groups [24]. These groups play a key role in the photoreactive process and then this dehydroxylation should be responsible for the deactivation observed in the catalytic runs carried out in the absence of water vapour.

3.5. Mechanistic aspects

The photo-oxidation runs indicated that toluene degradation occurred via the formation of various intermediates but significant differences exist between the gas–solid and the liquid–solid system, due to the key role played by the interfaces. In the table the intermediates found in both systems are reported. It can be noticed that the main intermediates found in significant amounts were *p*-cresol and benzaldehyde in the liquid–solid regime but only benzaldehyde in the gas–solid one by using both types of catalysts. In liquid–solid regime traces of other intermediates were also found: benzyl alcohol and pyrogallol were detected for both catalysts. Moreover, benzoic acid, hydroquinone and *trans*, *trans*-muconic acid were detected only with TiO_2 Merck. In gas–solid system benzyl alcohol and benzoic acid were found adsorbed on both catalysts. These findings suggest the occurrence of different photodegradation pathways not only depending on the interfaces but also on the kind of photocatalyst.

The formation of benzaldehyde and *p*-cresol and their subsequent photo-mineralisation together with the pathway of direct photo-mineralisation of toluene, can be roughly

described by the following reaction sequence:

$$TiO_2 + h\nu \rightarrow TiO_2(e_{cb}^-, h_{vb}^+) \quad (1)$$

$$O_{2(ads)} + e^- \rightarrow O_{2(ads)}^- \quad (2)$$

$$O_{2(ads)}^- + H_2O \rightarrow {}^\bullet OOH + OH^- \quad (3)$$

$$OH_{(surf)}^- + h_{vb}^+ \rightarrow {}^\bullet OH_{(surf)} \quad (4)$$

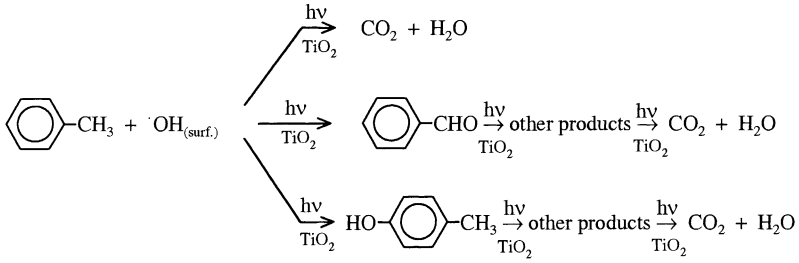

(5)

(6)

(7)

The presence of *p*-cresol only in the liquid–solid system indicates that a high concentration of water molecules would favour the attack to the toluene in the 4-position.

From the data reported in the table it can be observed that benzoic acid, as also other intermediate species detected in the liquid–solid system in the presence of TiO_2 Merck, was absent when TiO_2 Degussa P25 was used. This behaviour can be explained by considering the different interactions between the active sites of the solids and the adsorbed species. Indeed the absence of benzoic acid and other intermediates can be due to the high interaction of these molecules with the surface of the catalyst. The strong interaction of benzoic acid, highlighted by FTIR investigation, allows the subsequent degradation of this compound without its release to the liquid phase.

The last consideration can be also applied to justify the reactivity results obtained in gas–solid system. In fact the deactivation of TiO_2 Degussa P25 can be explained by taking into account the formation of photo-oxidised species strongly interacting with the surface and blocking the active sites; adsorbed emiacetalic species, precursors of carboxylate-like species, have been detected by FTIR investigation. The formation of unknown species cannot be excluded due to the presence of peaks (probably assignable to products with high molecular weight) in the HPLC chromatogram of the acetonitrile used to wash the photocatalyst at the end of the runs.

Differently from what observed in the gas–solid system where TiO_2 Degussa P25 deactivated even in the presence of water vapour, no deactivation was observed for both catalysts in the aqueous system. The presence of liquid water not only favours the desorption of intermediates but also produces restoration of the hydroxyl groups onto the surface.

Acknowledgements

The authors wish to thank the MIUR (Rome) for financial support. This work has been carried out in the framework of the Interuniversity Consortium “Chemistry for the Environment” (INCA, Italy).

References

[1] M. Schiavello (Ed.), Heterogeneous Photocatalysis, Wiley, New York, 1995.
[2] N. Serpone, E. Pelizzetti (Eds.), Photocatalysis: Fundamentals and Applications, Wiley, New York, 1989.
[3] A. Fujishima, K. Hashimoto, T. Watanabe, TiO_2 Photocatalysis: Fundamentals and Applications, BKC, Tokyo, 1999.
[4] V. Augugliaro, S. Coluccia, V. Loddo, L. Marchese, G. Martra, L. Palmisano, M. Pantaleone, M. Schiavello, Stud. Surf. Sci. Catal. 110 (1997) 663.
[5] J. Peral, D.F. Ollis, J. Catal. 136 (1992) 554.
[6] M.L. Sauer, D.F. Ollis, J. Catal. 158 (1996) 570.
[7] A.L. Linsebigler, G. Lu, J.T. Yates Jr., Chem. Rev. 95 (1995) 735.
[8] T. Ibusuki, K. Takeuchi, Atmos. Environ. 20 (1986) 1711.
[9] T.N. Obee, R.T. Brown, Environ. Sci. Technol. 29 (1995) 1223.
[10] Y. Luo, D.F. Ollis, J. Catal. 163 (1996) 1.
[11] H. Einaga, S. Futamura, T. Ibusuki, Appl. Catal. B 38 (2002) 215.
[12] V. Augugliaro, S. Coluccia, V. Loddo, L. Marchese, G. Martra, L. Palmisano, M. Schiavello, Appl. Catal. B 20 (1999) 15, and references therein.
[13] G. Martra, V. Augugliaro, S. Coluccia, E. García-López, V. Loddo, L. Marchese, L. Palmisano, M. Schiavello, Stud. Surf. Sci. Catal. 130 (2000) 665.
[14] L. Cao, Z. Gao, S.L. Suib, T.N. Obee, S.O. Hay, J.D. Freihaut, J. Catal. 196 (2000) 253.
[15] M. Fujihira, Y. Satoh, T. Osa, Nature 293 (1981) 206.
[16] M. Fujihira, Y. Satoh, T. Osa, J. Electroanal. Chem. 126 (1981) 1053.
[17] A. Navio, M. Garcia Gómez, M.A. Pradera Adrian, J. Fuentes Mota, J. Mol. Catal. 104 (1996) 329.
[18] V. Augugliaro, V. Loddo, G. Marcì, L. Palmisano, C. Sbriziolo, M. Schiavello, M.L. Turco Liveri, Stud. Surf. Sci. Catal. 130 (2000) 1973.
[19] R. Enriquez, P. Pichat, Langmuir 17 (2001) 6132.
[20] H. Tada, H. Matsui, F. Shiota, M. Nomura, S. Ito, M. Yoshihara, K. Esumi, Chem. Commun. (2002) 1678.
[21] G. Martra, Appl. Catal. A 200 (2000) 275.
[22] C. Morterra, A. Chiorino, F. Boccuzzi, E. Fisicaro, Z. Phys. Chem., Neue. Folge 124 (1981) 211.
[23] M. Nagao, Y. Suda, Langmuir 5 (1989) 42.
[24] G. Martra, S. Coluccia, L. Marchese, V. Augugliaro, V. Loddo, L. Palmisano, M. Schiavello, Catal. Today 53 (1999) 695.